Journal of Magnetism and Magnetic Materials 391 (2015) 156–160

Contents lists available at ScienceDirect

Journal of Magnetism and Magnetic Materials

journal homepage: www.elsevier.com/locate/jmmm

Multiferroicity in polar phase $LiNbO_3$ at room temperature

M. Manikandan [a], K. Saravana Kumar [b], N. Aparnadevi [a], N. Praveen Shanker [a], C. Venkateswaran [a,*]

[a] Department of Nuclear Physics, University of Madras, Guindy Campus, Chennai 600 025, India
[b] Department of Physics, SRM University, Ramapuram Campus, Chennai 600 089, India

ARTICLE INFO

Article history:
Received 19 November 2014
Received in revised form
4 April 2015
Accepted 26 April 2015
Available online 28 April 2015

Keywords:
Weak ferromagnetism
Ferroelectricity
Multiferroics

ABSTRACT

$LiNbO_3$, prepared by ball milling assisted ceramic method, exhibits weak ferromagnetism and ferroelectricity at room temperature. X-ray diffraction pattern reveals the rhombohedral phase of $LiNbO_3$ with hexagonal unit cell symmetry. The weak ferromagnetic behavior, obtained using VSM, has been explained using Dzyaloshinskii–Moriya interaction caused by the ferroelectric distortion in its magnetic order. The *P–E* loop measurement shows lossy natured ferroelectric loop. Electrical and dielectric properties analyzed using impedance spectroscopy show two thermally activated conduction processes, derived from the Arrhenius plot. A gradual increase in the dielectric constant below 493 K and a rapid increase above 493 K reveals the contribution of polarization components and Lithium ion hopping.

1. Introduction

$LiNbO_3$ with the space group R3*c* is *a* well known ferroelectric material and it exhibits excellent piezoelectric and pyroelectric properties based on its asymmetric structure [1]. Due to this $LiNbO_3$ has attracted extensive scientific and technological interest and has been widely used in many applications such as electro-optical, piezoelectrical and nonlinear optical devices [2]. Observation of magnetism along with ferroelectricity (Multiferroic behavior) in non-centrosymmetric polar phase of $LiNbO_3$ is anticipated to find applications in future generation novel devices. In the polar phase the Nb atom is displaced from the center of the oxygen octahedra sharing its faces along the trigonal polar axis. The next oxygen octahedra is empty and the one adjacent to it contains a Li atom displaced from the oxygen face, which results in the spontaneous polarization [3]. The displaced transition metal causes magnetic interactions through neighboring neutral oxygen vacancies. There are *a* few theoretical and experimental reports on the multiferroic response of $LiNbO_3$ [4–6] in which the authors have explained the experimentally observed ferromagnetism using oxygen vacancies [5,6]. The authors have theoretically suggested, using DFT calculation that in addition to the anion vacancies neutral cation vacancy also can cause ferromagnetism in $LiNbO_3$ [4]. However, investigation of electrical resistivity and dielectric behavior helps in the deep understanding of ferroelectricity in $LiNbO_3$. There are some reports on impedance studies of $LiNbO_3$ prepared by different methods like chemical evaporation, melt quenching and sol–gel methods [2,7,8]. To the best of our knowledge there is no report on temperature and frequency dependent dielectric properties of $LiNbO_3$ prepared by ball milling assisted ceramic method. Ball milling followed by heat treatment is a simple and efficient method where initial milling with optimum milling speed and time mechanically activates the precursors and thus reduces the phase formation temperature when compared to the solid state reaction method [9].

Therefore, $LiNbO_3$ has been synthesized using ball milling assisted sintering process. The observed weak ferromagnetism and ferroelectricity in $LiNbO_3$ are explained using Dzyaloshinskii–Moriya (DM) interactions and distortion of the centrosymmetry structure, respectively. Moreover, the dielectric properties are investigated over the temperature range of 400–650 K and frequency range of 100 Hz–1 MHz. The possible conduction mechanism and dipole orientations with respect to temperature and frequency are also discussed.

2. Experimental

Lithium carbonate (Li_2CO_3) and niobium oxide (Nb_2O_5) powders were taken in stoichiometric ratio, milled for 5 h at 250 rpm using zirconia vials and balls with a ball to powder ratio of 8:2. The milled powders were pressed into dense pellets of 12 mm diameter and sintered at 923 K in air for 6 h, subsequently furnace-cooled to room temperature. The sintered pellets were finally ground in a mortar to obtain $LiNbO_3$ powder.

---

* Corresponding author. Fax: +91 4422353309.
E-mail address: cvunom@hotmail.com (C. Venkateswaran).

http://dx.doi.org/10.1016/j.jmmm.2015.04.099
0304-8853/

X-ray diffraction (XRD) was carried out using Cu-Kα radiation for phase identification. High-resolution scanning electron microscopy (HR-SEM) was done in a FEI Quanta FEG 200 h microscope to study the surface morphological features. The ferroelectric loop was traced using Radiant Technologies Precision 4 kV HVI instrument. Isothermal magnetization curves up to a maximum field of ± 15 kOe were obtained in a Lakeshore VSM 7410 instrument. Dielectric measurements were done using an impedance spectrometer (Solartron impedance analyzer SI 1260) in the frequency range of 100 Hz–1 MHz and in the temperature range of 400–630 K.

3. Results and discussion

3.1. Structural and surface morphological studies

The diffraction pattern of $LiNbO_3$ indicating the single-phase nature with rhombohedral (trigonal) structure is shown in Fig. 1. Generally, trigonal systems can have two different symmetry viz, rhombohedral or hexagonal with an acentric space group $R3c$ [10]. The refinement is good with hexagonal polar symmetry and $R3c$ space group (No 161). The refined cell parameters $a=5.144(4)$ Å, $c=13.83(3)$ Å and, the corresponding cell volume $V=317$ Å^3 closely match with the JCPDS file no. 20-0631.

Surface morphological and microstructural features are shown in Fig. 2(a) and (b). Fig. 2(a) shows the homogeneous distribution of spherical shaped particles along with agglomerated islands at few places. The particle size is in the range 102–240 nm as shown in Fig. 2(b).

3.2. P–E loop measurement

The room temperature polarization–electric field (*P*–*E*) loop reveals the lossy natured ferroelectric behavior and is shown in Fig. 3. The observed lossy nature is due to the oxygen vacancies created during synthesis. The oxygen vacancies may suppress the dipole formation due to the deficiency in the charge densities, i.e. unequal amount of positive and negative charges. This leads to low resistivity and high leakage current in the presence of applied electric field leading to the lossy nature. The stoichiometry of oxygen was calculated using iodometric titration [11–13]. The titration was performed on 10 mg of prepared $LiNbO_3$, thrice. An excess of potassium iodide (KI) was dissolved in boiled distilled water. The solution containing KI and $LiNbO_3$ was made acidic by the addition of 3 N hydrochloric acid. The solution was titrated with standardized sodium thiosulfate (0.05 N). Standardization of sodium thiosulfate was done using potassium dichromate and starch was used as indicator. The estimated oxygen stoichiometry is 2.85 ± 0.01. The ferroelectricity in $LiNbO_3$ is due to the structural distortion of paraelectric centrosymmetric phase into the acentric polar phase as a function of temperature. In the paraelectric phase above the Curie temperature, the Li atoms lie in an oxygen layer that is $c/4$ distance away from the Nb atom, and the Nb atoms are centered between oxygen layers. These positions make the paraelectric phase (non-polar) [14]. The structure of paraelectric phase is shown in Fig. 4(a). As the temperature decreases below the Curie temperature, the elastic forces of the crystal become dominant, driving the lithium and niobium ions into new positions. The charge separation resulting from this shift of ions along c direction relative to the oxygen octahedral, shown in Fig. 4(b), causes the spontaneous polarization. The value of remanent polarization $P_r=0.09$ μC/cm^2 and saturation polarization $P_s=0.21$ μC/cm^2 obtained from the loop are close to the value reported by Díaz-Moreno et al. [5].

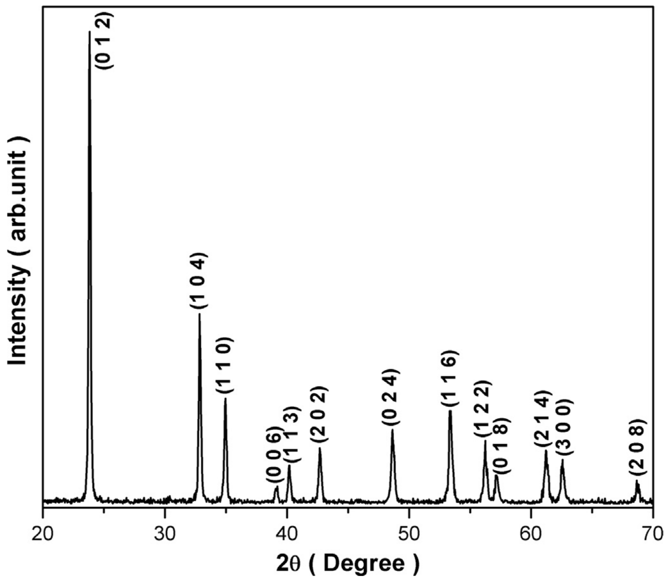

Fig. 1. X-ray diffraction pattern of $LiNbO_3$.

3.3. Magnetic study

Fig. 5 shows the magnetization curve of $LiNbO_3$ at room temperature. A weak ferromagnetic nature is observed with a saturation magnetization (M_s) of 0.02 emu/g and coercivity (H_c) of 415 Oe. The obtained M_s is close to the value (0.017 emu/g) reported for nanocrystalline $LiNbO_3$ but the value of H_c is small when compared to the value (750 Oe) reported for the nanocrystalline $LiNbO_3$ [5]. This can be attributed to the growth of larger particles i.e., as the particle size increases the coercivity decreases. During the synthesis process some of the neutral oxygen is expected to escape from the sample in the form of O_2 gas, resulting in the loss of acceptor charges which leads to the extended state of Nb-*s* electron in $LiNbO_3$. The asymmetric nature of electron spins (i.e., spin up and spin down) in Nb-*s* orbitals contribute to the magnetic property since there is no magnetically active ion. In the paraelectric phase the midpoint between two neighboring Nb ions act as an inversion center. In this case the spin of Nb-*s* electrons are arranged antiparallel to each other resulting in an antiferromagnetic coupling between Nb–Nb. This is energetically more favorable through the created oxygen vacancies [4]. This antiferromagnetic interaction is destroyed by the ferroelectric distortion, i.e displacement of Nb breaks the inversion center between the Nb ions and hence creates *a* small canting between the magnetic moments (i.e., a small deviation from overall spin configuration illustrated in Fig. 6) of neighboring Nb ions. The exchange interaction called as DM interaction [15] between the canted spins gives rise to a small net magnetization in the prepared polar (ferroelectric) phase $LiNbO_3$ and hence *a* weak ferromagnetism is observed. This kind of phenomena was also observed in $R3c$ $FeTiO_3$ [16] which is structurally isomorphic to $LiNbO_3$ polar phase.

3.4. Impedance spectroscopy

The dc resistivity plot is shown in Fig. 7. The resistivity values were extracted from the Z′ Vs Z″ plot. A gradual decrease in resistivity with temperature is observed. The conductivity is $3.5 \times 10^{-7}\ \Omega^{-1}\ cm^{-1}$ at 373 K and it increases to $3 \times 10^{-4}\ \Omega^{-1}\ cm^{-1}$ at 663 K. The order of obtained conductivity is higher than that of single crystal $LiNbO_3$ [17]. It was found that the ionic conductivity of $LiNbO_3$ increases while going from single crystalline nature to microcrystalline, nanocrystalline and amorphous [8].

The conduction mechanism is furthermore explained by the